

Properties of the He I 10830 Å Line in Solar Flares *

Qiu-Sheng Du and Hui Li

Purple Mountain Observatory, Chinese Academy of Sciences, Nanjing 210008, China; duqs@pmo.ac.cn

Received 2008 February 4; accepted 2008 April 21

Abstract We study the properties of the He I 10830 Å line in nine selected solar flares, using spectral data obtained with the Multi-channel Infrared Solar Spectrograph (MISS) at Purple Mountain Observatory (PMO) and photospheric images from the Michelson Doppler Imager (MDI) onboard the Solar and Heliospheric Observatory (*SOHO*). Our results indicate that, over an area of $3''$ – $8''$, the He I 10830 Å line shows emission exceeding the continuum in nearby quiet region when the Geostationary Operations Environmental Satellite (*GOES*) X-ray class of the flare reaches a threshold value (C4.5). The He I 10830 Å line emission is detected only in the kernels of the $H\alpha$ brightenings, but is not associated with the size of the flare. It is found that, whenever the He I 10830 Å line shows excess emission over the nearby continuum both the $H\alpha$ and the Ca II 8542 Å lines display enhanced intensities exceeding their preflare intensities. The He I 10830 Å line emission can occasionally extend into the umbra of the involved sunspot, which is inconsistent with previous studies. The weak component of He I 10830 Å line changes from emission to absorption earlier than does the main component. Our results favor the photoionization-reconnection mechanism for the excitation of the He I 10830 Å line.

Key words: Sun: flares — Sun: infrared — line: profiles

1 INTRODUCTION

Solar flare is one of the most energetic phenomena occurring in the solar atmosphere, and its spectrum provides important information for diagnosing its physical states. In addition to providing detailed information on the flaring plasma, including element abundance, turbulent velocity, electron temperature and density (e.g., Suemoto & Hiei 1959; Švestka 1976; Li et al. 2002a; Gu et al. 2003), high-resolution flare spectra can also provide unambiguous information on the dynamics of individual solar structures (Mariska 1994; Bentley et al. 1996; Brosius 2001; Morimoto & Kurokawa 2003; Qiu & Dare 2003).

The most studied spectral line of solar flares is the $H\alpha$ line. Following the development of the chromospheric condensation theory (Canfield 1986), Canfield & Gayley (1987) computed the $H\alpha$ profiles during the first few seconds of the heating of the chromosphere by non-thermal electron beams. The results indicated that one could determine whether a chromospheric flare is due to thermal conduction or non-thermal electron beams by measuring the red-shift and scrutinizing the shape of the $H\alpha$ line profile. This was challenged by later observational and theoretical works, which showed that large broadenings are also present in chromospheric lines of other elements, such as He I 10830 Å (e.g., You et al. 2001; Ding et al. 2005; Li et al. 2005, 2006, 2007) and Ca II 8542 Å (e.g., Ding et al. 1999; Fang et al. 2000; Li et al. 2005, 2007) lines. The Non-LTE calculation also suggested that the He I 10830 Å line could be a potential diagnostic tool for non-thermal effects in solar flares because the presence of non-thermal electron beam can significantly increase the strength of He I 10830 Å emission in a hot atmosphere (Ding et al. 2005).

* Supported by the National Natural Science Foundation of China.

The infrared triplet of neutral helium, He I 10830 Å, has a much higher excitation potential than hydrogen and Ca II, which makes it a special diagnostic tool for studying the hotter and denser flare atmosphere (Lites et al. 1986). Moreover, the absorption of the He I 10830 Å line is rather less than the H α line on the solar disk, therefore, it can observe a lower part of the flare than the H α line when the flare occurs near the solar limb. Meanwhile, the He I 10830 Å line profiles can be used to diagnose the structure of flare plasma and to test flare models (Li et al. 2006; Li et al. 2007). This triplet involves a metastable level (~ 20 eV above the ground state) as its lower level. However, the population of the metastable level remains an open question. So far, the photoionization recombination mechanism (PRM) and the collisional mechanism (CM) have been proposed to address this problem, but it is difficult to distinguish these two mechanisms and more work need to be done.

Many solar flares were observed in the H α , Ca II 8542 Å and He I 10830 Å lines with the Multi-channel Infrared Solar Spectrograph (MISS) (Li et al. 1999, 2002b) at Purple Mountain Observatory (PMO) in the 23rd solar cycle. In this paper, we have selected nine flares (five *GOES* M-class flares and four C-class flares), for which we have rather complete data sets, to further study the properties of the He I 10830 Å line, and compare with the H α and Ca II 8542 Å lines. The basic data of these flares are listed in Table 1. In the following sections, we show the observations and data reduction in Section 2, then present our results in Section 3, and finally give our discussion and summary in Section 4.

Table 1 List of the Studied Flares

| Observation Date | Flaring Time (UT) | | | NOAA | Flare Location | Flare Class | X-Ray Class | | Umbra/ Penumbra |
|---------------------|-------------------|-------|-------|-------|-------------------|----------------|-------------|------|--------------------|
| | Onset | Peak | End | | | | XRCA | XRCB | |
| 2001/11/07 | 01:39 | 01:46 | 01:52 | 9690 | S18E54 | 1F/M1.1 | M1.0 | C2.0 | umbra |
| 2001/11/09 | 05:20 | 05:39 | 05:48 | 9690 | S18E25 | 1F/M3.1 | M2.3 | C3.0 | penumbra |
| 2001/11/24 | 07:20 | 07:32 | 07:48 | 9704 | S18W56 | 1N/C5.8 | C2.4 | C1.8 | penumbra |
| 2001/12/21 | 05:16 | 05:21 | 05:27 | 9742 | N13E12 | SF/C4.0 | N/A | C1.7 | out of spot |
| 2001/12/24 | 02:59 | 03:04 | 03:10 | 9742 | N11W30 | SF/C3.3 | N/A | C1.8 | penumbra |
| 2001/12/29 | 05:40 | 05:45 | 05:50 | 9751 | N02W32 | 1F/M1.1 | M1.0 | C9.0 | out of spot |
| 2002/07/24 | 03:17 | 03:21 | 03:24 | 10039 | S16E59 | SF/C4.5 | C3.8 | C2.3 | penumbra |
| 2002/07/29 | 02:29 | 02:38 | 02:46 | 10044 | S20W14 | 1F/M4.8 | M1.1 | C3.0 | penumbra |
| 2003/10/23 | 07:02 | 07:08 | 07:10 | 10484 | N04E13 | 1N/M3.2 | M1.0 | C4.0 | penumbra |

2 OBSERVATIONS AND DATA REDUCTION

All the spectral data used in this study were obtained with the MISS at PMO. The solar image can be moved across the slit by rotating the second mirror of the coelostat system. We generally use the slit-pointing observing method for these flares. Photospheric images from the Michelson Doppler Imager (MDI) onboard Solar and Heliospheric Observatory (*SOHO*) together with the slit-jaw H α images from MISS are used to determine the relative location of the H α ribbons with respect to the relevant sunspots. Soft X-ray (SXR) data are from the Geostationary Operations Environmental Satellite (*GOES*).

MISS observations consist of the spectra in the three lines, H α , Ca II 8542 Å and He I 10830 Å, and H α images obtained simultaneously by the slit-jaw system, which uses a Daystar filter with a 0.5 Å passband. The integration times of the H α , Ca II 8542 Å and He I 10830 Å spectra are, respectively, 0.06 s, 0.1 s and 0.4 s, and the spectral dispersions are 0.05453 Å, 0.05113 Å and 0.04776 Å per pixel, respectively. The spatial resolution is 1.34'' along the slit after a 4-row binning, and the temporal resolution is about 2.8 s. The interference fringes of the back-illuminated CCD in the infrared waveband can hardly be removed completely, therefore they more or less affect the signal-to-noise ratio of the He I 10830 Å line. The observed spectral data are first corrected for dark-current, flat-field, scattered light, instrumental profile, and then are absolutely calibrated. Calibration is done by comparing the observed profiles in a nearby quiet region with the theoretical mean profiles for H α (David 1961) and Ca II 8542 Å (Linsky et al. 1970), with an observed standard profile for He I 10830 Å from BASS2000 (<http://bass2000.obspm.fr/>).

3 RESULTS

Here, we first introduce our method, using the 2001 November 7 flare as example, and then present our results on the location of the He I 10830 Å emission patches, time profiles of the He I 10830 Å line-center intensity, relation between the He I 10830 Å line emission and *GOES* X-ray class.

3.1 Method

The slit-jaw H α images of MISS were recorded with a Mintron MTV-1881EX B/W CCD, which has only 8-bit output. The recorded images have a pixel resolution of about 0.93'' (Li et al. 2002b). We planned to study the property of the He I 10830 Å line both in and outside the H α flare kernels, defined as the region of the slit-jaw H α image with brightness above 98% of the maximum brightness of the whole image. We then selected one representative point inside and one outside of the defined kernel of each flare for the line profile study. An example is given in Figure 1(a), in which the two arrows 'A' and 'B' mark the inside and outside points.

The He I 10830 Å triplet consists of the main (I_{12} , 10830.341 Å + 10830.250 Å) and the weak (I_3 , 10829.081 Å) components. The main component actually includes two components, which are blended and can hardly be separated. However, we can easily distinguish the main and the weak components if the flare is not too strong and the profile is not greatly broadened ($\Delta\lambda_D < 0.5$ Å) (You et al. 1998; Li & You 2001; You et al. 2004), which is the case for the selected flares here.

To determine the location of the He I 10830 Å emission patches with respect to the associated sunspot, we used photospheric intensity images from the MDI onboard the *SOHO*. The slit-jaw H α image and the MDI intensity image were carefully aligned using common features such as sunspots. We select a cut along the slit (indicated by the two white horizontal bars in Fig. 1(a)), and plot the normalized photospheric brightness (B_{ph}) and the ratio (R_{12}) of the line-center intensity of the main component of He I 10830 Å line (I_{12}) to the continuum (I_c) in a nearby quiet region along the cut in Figure 1(b). The two selected points ('A' and 'B') are indicated by the two vertical dotted lines, and the division of the umbra and penumbra of the sunspot by a horizontal line. We use the intensity ratio $R_{12} = I_{12}/I_c$, I_c being the continuum intensity in a nearby quiet region ($R_{12} > 1$ is called 'excess emission' for simplicity). Similarly, R_3 , R_{6563} and R_{8542} are for the I_3 components of the He I 10830 Å line, H α and Ca II 8542 Å lines, respectively.

Our spectroscopic observations were done with the slit pointing method, and during the observation the observer could move the slit to other locations to trace some specific features. Therefore, to study the time profile of the line intensity for a specific location, we need to ensure that the intensities are retrieved from the profiles taken at the same location. This is achieved by carefully comparing the slit-jaw H α images from MISS at different times. Based on this comparison, we select spectrograms in the He I 10830 Å, H α and Ca II 8542 Å lines, which are used to retrieve the line profiles. The line-center intensity of the two components of the He I 10830 Å line, and that of the H α and Ca II 8542 Å lines, are then calculated from the retrieved profiles after the absolute calibration, taking into account the possible line-center shift due to the line-of-sight (LOS) velocity of the flare plasma. Figure 2 shows a sample set of the He I 10830 Å, H α and Ca II 8542 Å line profiles for the 2002 July 7 flare at 03:22:06 UT taken with MISS. The short dashed vertical bars indicate the wavelengths where the line-center intensities were retrieved for the He I 10830 Å ($I_{12} + I_3$), H α and Ca II 8542 Å lines.

3.2 Brightening Patches in He I 10830 Å Line

From the example given in Figure 1, we see that the H α brightening covers a large part of the sunspot (Fig. 1(a)) and the He I 10830 Å line shows excess emission ($R_{12} > 1$, Fig. 1(b)) in a region of 3''–4''. Figure 1(b) also tells us that this region (with $R_{12} > 1$) extends into the umbra of the sunspot (with $B_{ph} < 0.64$). For the other eight flares, six of them show He I 10830 Å excess emission in a region of about 3''–8'', but none of such emission was detected in the umbra of the associated sunspot. No large sunspots are associated with the two flares occurred on 2001 December 21 and 29. One in a no sunspot region and another in a satellite sunspot region took place. In other words, among the nine flares, only in one case do we detect He I 10830 Å excess emission in the umbra of the sunspot. These results are listed in the last column of Table 1.

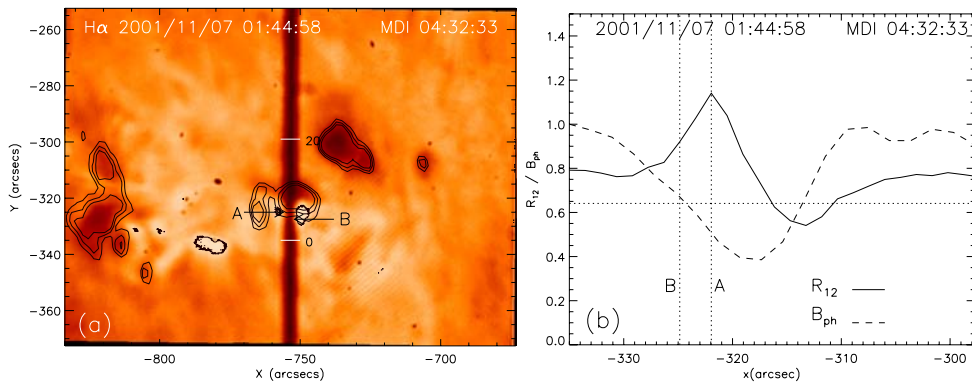


Fig. 1 (a) MISS slit-jaw $H\alpha$ image at 01:44:58 UT of 2001 November 7 overlaid with MDI intensity image (thin contour) at 04:32:33 UT. The thick contours show the $H\alpha$ kernels defined in the text. The dark vertical thick line stands for the slit of the spectrograph. The two arrows ‘A’ and ‘B’ mark the two points for which the line profiles are retrieved for the present study. The two short white horizontal bars marked ‘0’ and ‘20’ show the start and end locations of the cut along the slit for which the MDI brightness and the He I 10830 Å line-center intensity for the main component is plotted in panel (b). (b) Variations of the line-center intensity of the main component (I_{12}/I_c , solid line) of the He I 10830 Å profile and the normalized photospheric brightness (B_{ph} , dashed line) along the cut in panel (a). The two vertical dotted lines indicate the positions of the selected two points (‘A’ and ‘B’) shown in panel (a). The dotted horizontal line indicates the division of the umbra and penumbra of the sunspot.

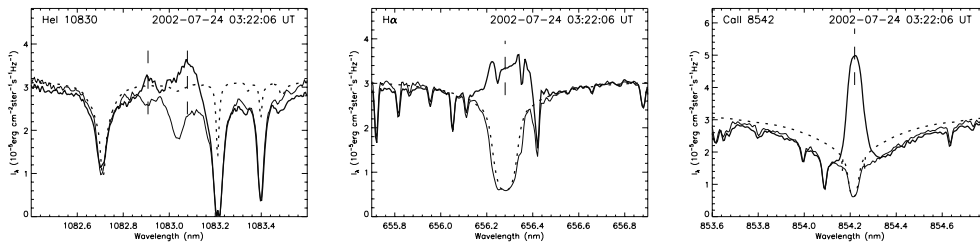


Fig. 2 Profiles of (a) He I 10830 Å, (b) $H\alpha$ and (c) Ca II 8542 Å lines for the 2002 July 24 flare at 03:22:06 UT from MISS observation. The dashed vertical bars indicate the wavelengths where the line-center intensities were retrieved. The thick/thin solid lines stand for the observed profiles in the flare and nearby quiet regions, respectively, while the dotted line for the theoretical ($H\alpha$ and Ca II 8542 Å) or observed (He I 10830 Å) standard profile.

3.3 Time Profiles of the He I 10830 Å Line-Center Intensity

Using the method described in Section 3.1, we derive the time profiles of the line-center intensities of the main and the weak components of the He I 10830 Å line, and those of the $H\alpha$ and Ca II 8542 Å lines for a point in the $H\alpha$ kernel (similar to point A in Fig. 1(a)) for each of the nine flares. The results for four of them together with the corresponding *GOES* 1 – 8 Å X-ray flux are plotted in Figure 3. From Figure 3 we notice that the components (I_{12} and I_3) of the He I 10830 Å line show similar variations with time even though I_{12} undergoes more obvious change during flare processes. Before the onset of the flare or in its early phase, the intensity of the main component is lower than the weak component. As the flare goes on and the triplet turns into emission, the intensity of the main component becomes higher than that of the weak (see, for example, Fig. 3(a)). From Figure 3(a) – (c) we see that the weak component of the He I 10830 Å line becomes absorption earlier than the main component if both two components show emission during the flaring process.

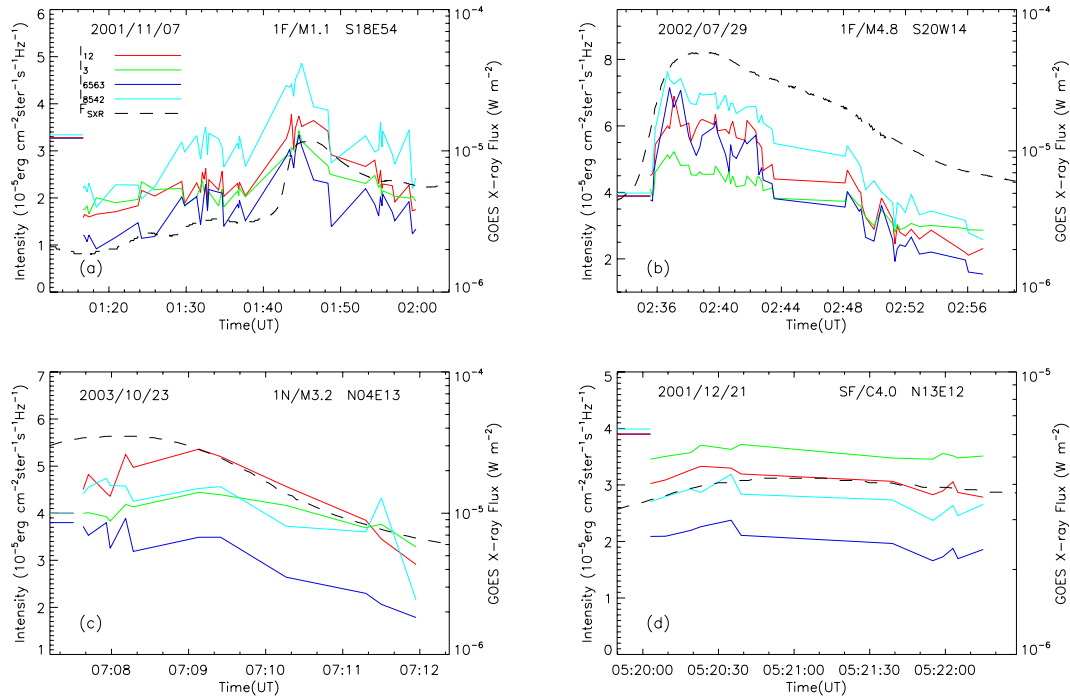


Fig. 3 Time profiles of the line-center intensities of the main (red) and the weak (green) components of the He I 10830 Å line, and those of H α (blue) and Ca II 8542 Å (cyan) lines for four of the studied flares together with the corresponding GOES X-ray 1 – 8 Å flux. The corresponding flare date, class and location are indicated in each panel. The horizontal bars on the left side of each panel indicate the continuum intensity in a nearby quiet region.

Our results show that the main component of the He I 10830 Å line shows excess emission in seven of the nine flares, and the maximum value of R_{12} is 1.77 in these flares. The H α and Ca II 8542 Å lines show excess emission in four and six flares, respectively. The maximum value of R_{6563} and R_{8542} is 1.69 and 1.82, respectively, which are from the same flare as the maximum R_{12} (i.e., the 2002 July 29 M4.8 flare). To be more clearly, we plot the maximum values of R_{12} , R_{6563} and R_{8542} in Figure 4 (we define the corresponding time as T_{\max}). We also plot in Figure 4 the values of R_{12} , R_{6563} and R_{8542} at the time (defined as $T_{R_{12}=1}$) when the main component of the He I 10830 Å line stops showing excess emission (denoted with R_{12C} , R_{6563C} and R_{8542C} , respectively). We can see from the figure that R_{6563C} and R_{8542C} vary significantly from case to case, suggesting that they are not obviously correlated to whether the He I 10830 Å shows excess emission.

To be more comprehensive, we compute the intensity ratios of the H α line, Ca II 8542 Å line and the main component of He I 10830 Å line at different times for each flare during the flare process for two points, that one of which is in and another is out of the H α kernel (similar to point A and B in Fig. 1(a)). The results are plotted in Figure 5, which shows that the He I 10830 Å line indicates no excess emission in all the flares for the point out of the H α kernel. Actually, a careful comparison of the He I 10830 Å line-center intensity with the continuum intensity of the flare itself implies that the He I 10830 Å displays no emission out of the H α flare kernels. Indeed, the emission in the H α line is also weak out of the H α flare kernels and no excess emission is detected. However, in contrast to the He I 10830 Å line, the Ca II 8542 Å line shows more or less emissions out of the H α flare kernels (Fig. 5) as demonstrated by the triangles with $R_{8542} > 1$ in Figure 5(b). On the other hand, both the H α and the Ca II 8542 Å lines display emissions wherever the

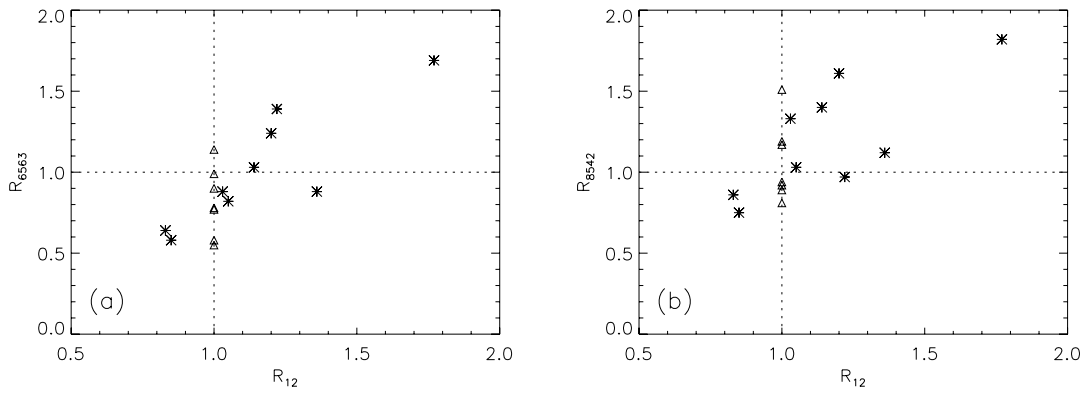


Fig. 4 Scatter plot of the intensity ratio variations of (a) $H\alpha$ and (b) $\text{Ca II } 8542 \text{ \AA}$ lines with that of the I_{12} component of the $\text{He I } 10830 \text{ \AA}$ triplet at T_{max} (asterisk) and $T_{R_{12}=1}$ (triangle).

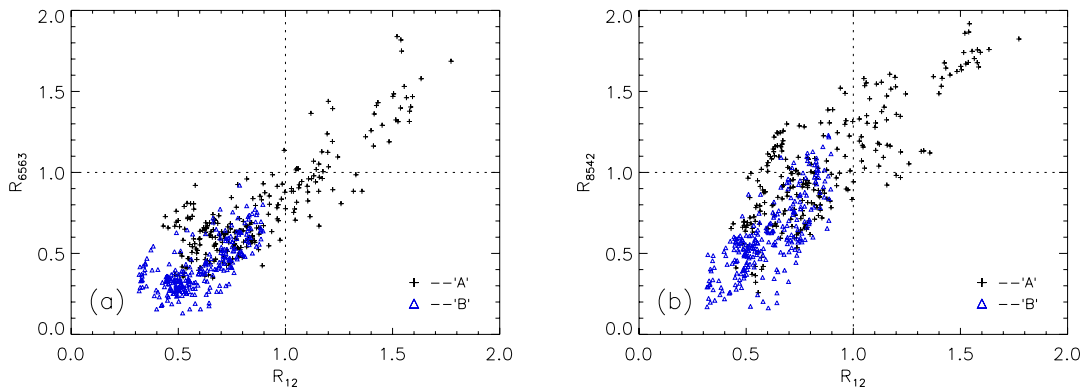


Fig. 5 Scatter plot of the intensity ratio variations of (a) $H\alpha$ and (b) $\text{Ca II } 8542 \text{ \AA}$ lines with that of the I_{12} component of the $\text{He I } 10830 \text{ \AA}$ triplet at different times in the flaring process for the selected point in the $H\alpha$ kernel (plus) and the point out of the $H\alpha$ kernel (triangle).

$\text{He I } 10830 \text{ \AA}$ line shows emission, even though they may be lower than the continuum in a nearby quiet region.

3.4 Relation between the $\text{He I } 10830 \text{ \AA}$ Line Emission and *GOES* X-Ray Flux

To check the relation between the $\text{He I } 10830 \text{ \AA}$ line emission and the *GOES* X-ray flux, we plot the variation of the intensity ratio of the I_{12} component of the $\text{He I } 10830 \text{ \AA}$ triplet with the corresponding *GOES* 1–8 \AA X-ray flux of each flare at T_{max} ($R_{12\text{max}}$) and $T_{R_{12}=1}$ (R_{12C}) in Figure 6(a) and (b), respectively. The corresponding values for the $H\alpha$ and the $\text{Ca II } 8542 \text{ \AA}$ lines are also plotted in the figure for comparison. The figure shows that, generally, the maximum intensity ratio $R_{12\text{max}}$ of the $\text{He I } 10830 \text{ \AA}$ line increases with the *GOES* X-ray class, i.e., the $\text{He I } 10830 \text{ \AA}$ line emission is related to the strength of X-ray emission. Figure 6(a) indicates that when the *GOES* X-ray class increases to C4.5 (as indicated by the dashed vertical line in panel (a)), the $\text{He I } 10830 \text{ \AA}$ line shows excess emission during the flaring process while the $H\alpha$ and $\text{Ca II } 8542 \text{ \AA}$ lines may not (see the points in the region defined by $R_{\text{max}} < 1$ and *GOES* X-ray class $> \text{C4.5}$

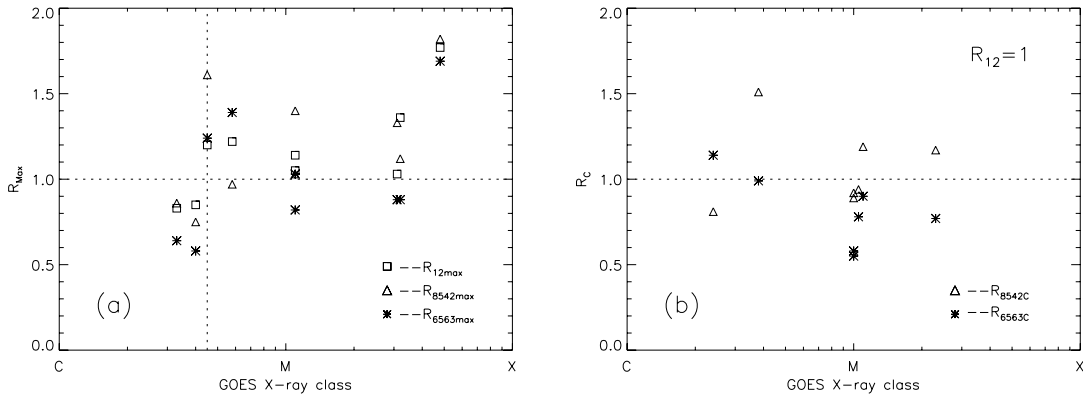


Fig. 6 Scatter plot of line intensity ratio (R) of the $H\alpha$ (asterisk), Ca II 8542 Å (triangle) and I_{12} component of He I 10830 Å (square) lines for the studied flares with *GOES* X-ray class (a) at T_{\max} , and (b) at $T_{R_{12}=1}$.

in Fig. 6(a)). When the X-ray class is less than C4.5, the He I 10830 Å line displays only weak emission (less than the nearby continuum).

We retrieve the information of *GOES* X-ray flux when the He I 10830 Å line started to show excess emission if we observed the initial phase of the flare or when it stopped showing excess emission if our observation missed the initial phase. The X-ray class obtained in this way (we call it ‘XRCA’) for each flare is listed in Table 1 (also see Fig. 6(b)) together with the background X-ray class (XRCB). From Table 1 we see that the XRCA varies significantly from case to case (from C2.4 to M2.3), and is positively correlated to the X-ray class of the flare. No apparent correlation is found between XRCA and XRCB.

4 DISCUSSION AND SUMMARY

We have studied the He I 10830 Å line profiles of nine solar flares. The He I 10830 Å line in solar flares displays unique spectral properties. Our results show that its intensity is not associated with the area (optical class) of the flare or the intensity of the $H\alpha$ line (Figs. 4 and 5) but is associated with the X-ray intensity (Fig. 6). It is only when the *GOES* X-ray flux reaches a certain threshold (C4.5 in this paper), that excess emission is detected in this line, in a limited region of $3'' - 8''$, corresponding to some bright $H\alpha$ kernel. This is consistent with the previous studies (You et al. 1993; Li et al. 2007) but the threshold found here is slightly lower than their value (C6.0).

The He I 10830 Å line appears in absorption when the *GOES* X-ray flux is below the threshold, and so appears in regions outside of the $H\alpha$ kernels even when the *GOES* X-ray flux exceeds the threshold (Figs. 5 and 6). The corresponding X-ray classes are C2.3 and C4.5, respectively, for the 2002 July 24 C4.5 and 2001 November 24 C5.8 flares when the He I 10830 Å line shows the maximum excess emission. Namely, the excess emission of the He I 10830 Å line can be detected at an X-ray level lower than C4.5 if the X-ray class of the flare is higher than this value, but this is not associated with the background X-ray flux before the flare. According to the previous studies, EUV loops of solar flares may be formed by cooling the X-ray loops (e.g., Warren et al. 2002; Spadaro et al. 2003), so strong X-ray emission in a solar flare suggests a strong EUV emission. Therefore, our results tend to favor the PRM for the excitation of the He I 10830 Å line. The PRM assumes that corona EUV emission leads to the over-ionization of neutral helium in the chromosphere, followed by recombination to the excited levels. Therefore, the He I 10830 Å line can reflect the X-ray emission strength in the corona above a flare and can provide observational data to diagnose the excitation mechanisms of the helium lines (Li et al. 2007).

We notice that the $H\alpha$ and Ca II 8542 Å lines may not show excess emission even when the *GOES* X-ray class reaches the threshold (Fig. 6). This is possibly because the $H\alpha$ and Ca II 8542 Å lines are formed in different layers and by different mechanisms. As mentioned above, the He I 10830 Å line is mainly due to the PRM excitation, and its intensity is positively correlated to the EUV emission in the corona. In

contrast, the intensities of the $H\alpha$ and $Ca\ II\ 8542\ \text{\AA}$ lines are primarily determined by the heating level of the chromosphere. Therefore, different heating mechanisms of the corona and chromosphere will result in the above observational differences in the three lines.

In one of the nine flares (2001 November 7 flare), we detected the $He\ I\ 10830\ \text{\AA}$ line emission in the umbra of the sunspot. That means, like the $H\alpha$ and $Ca\ II\ 8542\ \text{\AA}$ lines, $He\ I\ 10830\ \text{\AA}$ line can sometimes in emission also in the umbra of sunspots. This is inconsistent with the previous result (Li et al. 2007), that $He\ I\ 10830\ \text{\AA}$ emission was only detected in the kernel of the $H\alpha$ brightenings. We did not detect any emission in the $He\ I\ 10830\ \text{\AA}$ line (Fig. 5) in the $H\alpha$ kernels, although the $Ca\ II\ 8542\ \text{\AA}$ line may show some emission there. This means the bright regions of solar flares are much smaller in $He\ I\ 10830\ \text{\AA}$ than in $H\alpha$ or $Ca\ II\ 8542\ \text{\AA}$. Nevertheless, whenever $He\ I\ 10830\ \text{\AA}$ line showed excess emission over the nearby continuum we detected enhanced intensity in both $H\alpha$ and $Ca\ II\ 8542\ \text{\AA}$ lines, exceeding their preflare values.

The time profiles of the line-center intensities of the three lines underwent similar variations in time, which probably implies that they were formed in not too different environments. The line-center intensities of the main and the weak components of the $He\ I\ 10830\ \text{\AA}$ line also showed similar temporal behavior, but the weak component became absorption earlier than the main component, presumably due to its smaller optical thickness, making it to originate further down in the solar atmosphere. In other words, when the weak component starts to reflect the information of the cooler atmosphere below the flaring plasma the main component still mainly comes from the hot flaring plasma.

We notice that there are fluctuations in the time profiles of the line-center intensities shown in Figure 3. This is mainly due to the effect of varying seeing during the observations, and mis-alignment of the slit-jaw $H\alpha$ images, etc. However, these should not affect our results. It is worth mentioning that the X-ray threshold (C4.5) for the $He\ I\ 10830\ \text{\AA}$ line to show excess emission was based on nine flares and we need to check more flares to give a more precise determination: this will be done in the near future.

In summary, the $He\ I\ 10830\ \text{\AA}$ line shows excess emission when *GOES* X-ray class of the flare reaches the C4.5 threshold value. This event is not associated with the area of the flare, and can occasionally take place in the umbra of the sunspot. Meanwhile, $He\ I\ 10830\ \text{\AA}$ emission is detected only in kernels of $H\alpha$ brightenings. The weak component of the $He\ I\ 10830\ \text{\AA}$ line changes from emission to absorption earlier than does the main component. Our results seem to support the PRM for the $He\ I\ 10830\ \text{\AA}$ line excitation.

Acknowledgements This work was supported by the National Natural Science Foundation of China (Grant Nos. 10573038 and 10333040), the National Basic Research Program of China (2006CB806302), the CAS Project (KJCX2-YW-T04), and the China Meteorological Administration Grant (GYHY200706013).

References

- Bentley R. D., Doschek G. A., Mariska J. T., 1996, *Adv. Space Res.*, 17, 55
 Brosius J. W., 2001, *ApJ*, 555, 435
 Canfield R. C., 1986, In: R. F. Neidig, ed., *The Lower Solar Atmosphere of Solar Flares*, NSO/Sunspot, New Mexico, p.10
 Canfield R. C., Gayley K. G., 1987, *ApJ*, 322, 999
 David K. H., 1961, *ZAp*, 53, 37
 Ding M. D., Fang C., Yin S. Y., Chen P. F., 1999, *A&A*, 348, L29
 Ding M. D., Li H., Fang C., 2005, *A&A*, 432, 699
 Fang C., Hénoux J.-C., Ding M. D., 2000, *A&A*, 360, 702
 Gu X. M., Dun J. P., Zhong S. H., 2003, *New Astron.*, 8, 427
 Li H., Fan Z. Y., You J. Q., 1999, *Sol. Phys.*, 185, 67
 Li H., You J. Q., 2001, *A&A*, 374, 1121
 Li H., You J., Yu X. F., Wu Q. D., 2002a, *A&A*, 391, 741
 Li H., You J. Q., Wu Q. D., Yu X. F., 2002b, *Chin. Phys. Lett.*, 19, 742
 Li H., You J. Q., Du Q. S., Yu X. F., 2005, *Sol. Phys.*, 225, 75
 Li H., You J. Q., Du Q. S., 2006, *Sol. Phys.*, 235, 107
 Li H., You J. Q., Yu X. F., Du Q. S., 2007, *Sol. Phys.*, 241, 301
 Linsky J. L., Teske R. G., Wilkinson C. W., 1970, *Sol. Phys.*, 11, 374

- Lites B. W., Neidig D. F., Bueno J. T., 1986, In: F. F. Neidig, ed., The lower atmosphere of solar flares, NSO/Sunspot, New Mexico, p. 101
- Mariska J. T., 1994, *ApJ*, 434, 756
- Morimoto T., Kurokawa H., 2003, *PASJ*, 55, 505
- Qiu J., Gary D. E., 2003, *ApJ*, 599, 615
- Rust D. M., Bridges III C. A., 1975, *Sol. Phys.*, 43, 129
- Spadaro D., Lanza A. F., Lanzafame A. C., Karpen J. T., Antiochos S. K. et al., 2003, *ApJ*, 582, 486
- Suemoto Z., Hiei E., 1959, *PASJ*, 11, 185
- Švestka Z., 1976, *Solar Flares*, D. Reidel Publ. Co., Dordrecht, the Netherlands
- Warren H. P., Winebarger A. R., Hamilton, P. S., 2002, *ApJ*, 579, L41
- You J. Q., Wang C. J., Fan Z. Y., 1993, In: Proceedings of the First China-Japan Seminar on Solar Physics, G. X. Ai et al., eds., Kunming: Kunming Tondar Institute, p. 148
- You J. Q., Wang C. J., Fan Z. Y., Li H., 1998, *Sol. Phys.*, 182, 431
- You J. Q., Li H., Fan Z. Y., Sakurai T., 2001, *Sol. Phys.*, 203, 107
- You J. Q., Li H., Hiei E., 2004, *Sol. Phys.*, 223, 169